

Expression of the chemokine receptor CCR1 promotes the dissemination of multiple myeloma plasma cells *in vivo*

Mara N. Zeissig,^{1,2} Duncan R. Hewett,^{1,2} Vasilios Panagopoulos,^{1,2} Krzysztof M. Mroziak,^{1,2} L. Bik To,³ Peter I. Croucher,^{4,5} Andrew C.W. Zannettino^{4,2,6,7#} and Kate Vandyke^{1,2#}

¹Myeloma Research Laboratory, Adelaide Medical School, Faculty of Health and Medical Sciences, University of Adelaide, Adelaide, South Australia; ²Precision Medicine Theme, South Australian Health and Medical Research Institute, Adelaide, South Australia; ³Department of Hematology, Royal Adelaide Hospital, Adelaide, South Australia; ⁴Bone Biology Division, Garvan Institute of Medical Research, Sydney, New South Wales; ⁵St Vincent's Clinical School, Faculty of Medicine, University of New South Wales, Sydney, New South Wales; ⁶Central Adelaide Local Health Network, Adelaide, New South Wales and ⁷Center for Cancer Biology, University of South Australia, Adelaide, New South Wales, Australia.

#ACWZ and KV contributed equally as co-senior authors.

©2021 Ferrata Storti Foundation. This is an open-access paper. doi:10.3324/haematol.2020.253526

Received: March 25, 2020.

Accepted: October 23, 2020.

Pre-published: November 5, 2020.

Correspondence: KATE VANDYKE - kate.vandyke@adelaide.edu.au

Supplementary Methods

Flow cytometry on patient samples:

Ethical approval for this study was obtained from the University of Freiburg Medical Centre Ethics Review Committee and all patients provided written, informed consent, in accordance with the Declaration of Helsinki. Posterior superior iliac spine BM aspirates were collected in potassium EDTA tubes and mononuclear cells were isolated by density gradient centrifugation (Ficoll) and were cryopreserved prior to use, as described previously.¹ CCR1 analysis was on BM from 28 newly diagnosed MM patients that had not received previous therapy [median age: 68 years (range: 49–84); male:female ratio 1.15:1] and 7 patients with monoclonal gammopathy of undetermined significance (MGUS)² [median age: 74 years (range: 53–88); male:female ratio 1.7:1]. Cell surface CCR1 expression was assessed on viable CD38⁺/CD138⁺/CD45^{lo}/CD19⁻ malignant PC in MM and MGUS patients by multicolor flow cytometry (FACSARIA III; BD Biosciences, San Jose, CA) as previously described.³ CCR1 expression was quantitated as the change in the median fluorescence intensity (Δ MFI), defined as the difference in MFI between the CCR1-stained sample and the fluorescence minus one (FMO) control.

Patient microarray and RNA-sequencing analyses:

Analysis of the association between CD138⁺ BM PC expression of *CCR1*, known prognostic factors and overall survival was assessed in newly diagnosed MM patients (n=142) using Affymetrix GeneChip Human Genome U133 microarray dataset E-TABM-1138²⁸, from ArrayExpress (EMBL-EBI), as previously described.³ RNA-sequencing data from CD138-selected BM PC from a cohort of MM patients was obtained from the Multiple Myeloma Research Foundation (MMRF) CoMMpass (MMRF-COMMPASS) dataset, accessed via the NIH NCI GDC Data Portal (9 August 2019). Analysis was performed on data from MM patients (n=43) who had RNA-sequencing performed from a sample taken at diagnosis (baseline) and a sample taken following at least one line of therapy (subsequent). Patients were categorised as having low tumour *CCR1* expression (*CCR1* < 10 fragments per kilobase of transcript per million reads [FPKM] at both initial and subsequent biopsy; n=26; median age: 70 years [37–83]; male:female ratio 1.36:1), high *CCR1* (*CCR1* ≥ 10 FPKM at initial biopsy; n=7; median age: 66 years [39–70]; male:female ratio 1.31:1) or increased *CCR1* (initial *CCR1* < 10 FPKM and subsequent *CCR1* ≥ 10 FPKM; n=10; median age: 66 years [50–82];

male:female ratio 2.33:1). Median time between baseline and subsequent samples was 70.1 weeks [range: 8.4-202.7 weeks].

Reagents:

All reagents were sourced from Sigma-Aldrich (St Louis, MO) unless otherwise stated. Recombinant human (rh)CCL3 was sourced from R&D Systems (Minneapolis, MN). The small molecule CCR1 inhibitor CCX9588 was provided by ChemoCentryx (Mountain View, CA). For *in vitro* assays, CCX9588 was prepared at 2mM stock concentrations in DMSO and was stored at room temperature until use. Final DMSO concentration in all treatment media was 0.01%. For *in vivo* experiments, CCX9588 was prepared at 7.5mg/mL stock concentration in polyethylene glycol (PEG) vehicle and stored at room temperature until use.

Cell culture:

All media were supplemented with 2mM L-glutamine, 100U/ml penicillin, 100µg/ml streptomycin, 1mM sodium pyruvate and 10mM HEPES buffer, unless otherwise specified. The mouse MM cell line 5TGM1-luc (expressing a dual GFP and luciferase reporter construct)⁴ was maintained in Iscove's modified Dulbecco's medium (IMDM) with 20% foetal calf serum (FCS; HyClone, QLD, Australia) and supplements. HMCLs RPMI-8226-luc (expressing GFP/luciferase)⁵ and OPM2 were maintained in Roswell Park Memorial Institute Medium 1640 (RPMI-1640) with 10% FCS and supplements. All cell lines were cultured in a humidified environment with 5% carbon dioxide at 37°C.

Generation of 5TGM1 CCR1-expressing cell line:

5TGM1-luc genomic DNA was isolated using a DNeasy Blood and Tissue kit (Qiagen, Hilden, Germany) and used for amplification of the murine *Ccr1* gene by a nested polymerase chain reaction (PCR) using Phusion high-fidelity polymerase (New England Biolabs, Ipswich, MA). Primers in the first reaction were designed to flank the *Ccr1* coding sequence with a 5' BamHI restriction site and the beginning of the human influenza hemagglutinin (HA)-tag on the 3' end (nucleotide sequence of HA-tag: TATCCTTATGATGTTCCCTGATTATGCT) (Fwd 5'-GACCGGATCCTCAGCCCACCATGGAGATTTTCAGAT-3'; Rev 5'-TCAGGAACATCATAAGGATAGAAGCCAGCAGAGAGCTCAT-3'). In the second reaction, the same forward primer was used, with the reverse primer designed to overlap the first reverse primer to complete the HA-tag and add a 3' NotI restriction site (Rev 5'-TTGTGCGGCCGCCTAAGCATAATCAGGAACATCATAAGGATA-3'). The HA-tag was

used for protein expression confirmation by immunoprecipitation with an anti-HA-tag antibody (Sigma Aldrich, catalogue number 05-904), as previously described,⁴ and the restriction sites enabled cloning into pLeGOiCer2 lentiviral vector (gift from Boris Fehse⁶ Addgene #27346). 5TGM1-luc cells were infected with lentivirus as previously described.⁷ Briefly, for lentivirus production, HEK293T cells were transfected with pLeGOiCer2 or pLeGOiCer2-CCR1 (4µg), and packaging plasmids psPAX2 (4µg; gift from Didier Trono [Swiss Federal Institute of Technology Lausanne]; Addgene #12260) and pHCMV-EcoEnV (4µg; gift from Miguel Sena-Esteves⁸; Addgene #15802) using Lipofectamine-2000 (ThermoFisher). Lentiviral-supernatant was collected after 48 hours and 5TGM1-luc cells were infected with supernatant supplemented with 8µg/mL polybrene (Millipore, Burlington, MA). GFP and Cerulean-double-positive cells were sorted by FACS using a FACSAria™ Fusion flow cytometer (BD Biosciences, San Jose, CA) to generate a CCR1-expressing (5TGM1-CCR1) or EV control (5TGM1-EV) cell line.

Generation of OPM2 CCR1-knockout cell lines:

CCR1 knockout (KO) cell lines were generated using a lentiviral two-vector CRISPR-Cas9 system consisting of a Cas9 constitutive expression vector with an mCherry reporter (FuCas9Cherry; gift from Marco Herold, Addgene plasmid #70182⁹) and a doxycycline-inducible sgRNA expression vector with an eGFP reporter (FgHtUTG; gift from Marco Herold, Addgene plasmid #70183⁹) An mPlum FgH1tUTP vector was generated by digestion of the FgH1tUTG vector with BspI and ClaI to excise the *egfp* gene, which was replaced with a synthesised *mplum* gBlock gene fragment (Integrated DNA Technologies, Newark, NJ) using isothermal assembly. Two CRISPR strategies were used (Supplementary Figure 1). The MIT CRISPR design software (<http://crispr.mit.edu>) was used for the design of the sgRNAs. sgRNAs were designed to either flank the human CCR1 coding exon to delete the exon (sgRNA-A and sgRNA-B), or to target key tyrosine residues located in the ligand-binding domain (sgRNA-C). For cloning of individual sgRNAs, 24-bp oligonucleotides were synthesised (Sigma-Aldrich) including the sgRNAs sequences (gRNA-A 5'-GTTAGACTAAGATTCCTAGA-3'; gRNA-B 5'-GAGGGAATGTAATGGTGGCC-3'; gRNA-C 5'-GCCATGTGTAAGATCCTCTC-3') and 4-bp overhang for the forward (TCCC) and reverse (AAAC) oligonucleotides to enable cloning into the BsmBI site of the FgHtUT vectors.

OPM2 cells were first infected with FuCas9mCherry and FACS sorted for mCherry positive cells (OPM2-Cas9) using a FACS Aria™ Fusion flow cytometer. To generate empty vector control lines, OPM2-Cas9 cells were infected with the FgH1tUTG or FgH1tUTP vectors, alone, were sorted for mCherry⁺GFP⁺ (OPM2-EV-1) or mCherry⁺mPlum⁺ (OPM2-EV-2) cells, respectively. To generate gRNA-expressing cells, OPM2-Cas9 cells were either co-infected with the FgH1TUTG-sgRNA-A and FgH1TUTG-sgRNA-B vectors or were infected with the FgH1TUTP-gRNA-C vector alone.

For isolation of the clonal OPM2-CCR1-KO-1 cell line, OPM2-Cas9 cells transfected with FgH1TUTG-sgRNA-A and FgH1TUTG-sgRNA-B vectors were sorted into 96-well plates using a FACS Aria™ Fusion flow cytometer for single cell analysis. Clones were subsequently screened to identify CCR1-negative clones. Briefly, 1x10⁵ cells per test were stained with an anti-CCR1 mouse monoclonal antibody (clone 53504; R&D Systems) or an in-house IgG2B isotype control antibody (1A6.11), followed by a goat anti-mouse biotinylated secondary antibody (Southern Biotech, Birmingham, AL), followed by a BV421-conjugated streptavidin tertiary antibody (BD Biosciences, North Ryde, Australia). Cells were analysed using a LSRFortessa flow cytometer (BD Biosciences). Genomic DNA from the CCR1-negative clones was isolated using a DNeasy kit and 35 cycles of PCR was conducted using primers designed to flank the first coding exon of human CCR1 (Fwd 5'-TGGGGTTGACCTACTAGGATT-3'; Rev 5'-TCGCTGCAATAAAGCCATTAG-3') and the products subjected to agarose gel electrophoresis to identify whole exon deletions (Supplementary Figure 1B). Gel purified PCR products were subjected to Sanger sequencing (AGRF). This identified a clonal homozygous KO CCR1 cell line (OPM2-CCR1-KO-1) (Supplementary Figure 1C).

For isolation of the non-clonal OPM2-KO-2 cell line, OPM2-Cas9 cells transfected with FgH1tUTP-gRNA-C vector were stained with antibodies against CCR1, as described above, and sorted on the basis of mPlum⁺mCherry⁺BV421⁻ to isolate a CCR1-knockout population (OPM2-CCR1-KO-2). Mutagenesis was confirmed in the OPM2-CCR1-KO-2 line by conducting 35 cycles of PCR using primers flanking the CCR1 ligand binding domain (Fwd 5'-GCCTTTAGTAGCAGAGTAAAGACA-3'; Rev 5'-CCAGCCCAAAGAGGTTTCAGTT-3'). Reannealed PCR products were subjected to heteroduplex analysis by resolution on a 1xTBE polyacrylamide gel (Supplementary Figure 1E).

Quantitative real time PCR (qPCR):

Total RNA was isolated using TRIzol reagent (Thermofisher, Waltham, MA) and DNase treated using RQ1 DNase as per the manufacturer's instructions (Promega, Madison, WI). cDNA was synthesized using Superscript IV First-Strand Synthesis System (Thermofisher). Real-time PCR was performed using a Bio-Rad CFX 9000 qPCR instrument (BioRad, Hercules, CA) using primers for murine *Ccr1* (Fwd 5'-GTGGTGGGCAATGTCCTAGT-3'; Rev 5'-AGAAGCTTGACATGGCATC-3') and *Actb* (Fwd 5'-GATCATTGCTCCTCCTGAGC-3'; Rev 5'-GTCATAGTCCG CCTAGAAGCAT-3'). Changes in gene expression were calculated relative to *Actb* using the $2^{-\Delta\Delta C_t}$ method.¹⁰

Transwell migration assays:

For HMCLs, cells (1×10^5) were washed once in RPMI-1640 with 1% FCS and were seeded in 8 μ m transwells (Costar) in triplicate and cell migration towards rhCCL3 (100ng/mL) in RPMI-1640 with 1% FCS, or RPMI-1640 with 1% FCS alone (untreated controls) was assessed after 18 hours as previously described.³ Where indicated, cells were treated with CCX9588 (100nM-1 μ M) or vehicle control for 24 hours, then washed once in RPMI-1640 with 1% FCS and resuspended in RPMI-1640 with 1% FCS containing CCX9588 prior to seeding into transwells. For the murine MM PC cell line 5TGM1, cells (5×10^5) were washed once in IMDM with 1% FCS and were seeded in transwells in IMDM with 1% FCS in triplicate and cell migration towards IMDM with 20% FCS and rhCCL3 (100ng/mL) or IMDM and 20% FCS alone (untreated controls) was assessed after 24 hours using a luciferase assay, as previously described.⁴ The mean basal migration of cell lines was 0.1% (5TGM1), 0.3% (RPMI-8226) and 2.8% (OPM2). The observed intra-assay variation in basal migration was 53.4% (5TGM1), 18.6% (RPMI-8226) and 18.4% (OPM2) and the inter-assay variation was 60.9% (5TGM1), 47.3% (RPMI-8226) and 20.5% (OPM2). Percentage cell migration is represented as normalized to the untreated controls.

Proliferation assays:

Cells were plated at 1×10^5 cells/mL in triplicate in phenol red-free IMDM containing 20% FCS and supplements (5TGM1) or phenol red-free RPMI-1640 containing 10% FCS and supplements (OPM2-EV-1 and RPMI-8226-luc) with or without addition of rhCCL3 (100ng/mL) or CCX9588 (0.1nM-1 μ M) or vehicle, in a 96-well plate. Cell numbers were

assessed over 72 hours using WST-1 reagent (Roche, Basel, Switzerland) as previously described.¹¹

Western blotting:

For CCL3 stimulation experiments, OPM2-EV-1 or RPMI-8226-luc cells were treated with CCX9588 (10nM-10 μ M) or vehicle (0.01% DMSO) for 24 hours in serum-free RPMI-1640 containing supplements. Cells were stimulated with rhCCL3 (100ng/mL) for 5 min and cell lysates were prepared as previously described.¹² Proteins (50 μ g) were resolved under reducing conditions on 10% SDS-PAGE gels and transferred to 0.45 μ m nitrocellulose membranes. Immunoblotting was performed with the following antibodies: phosphorylated Akt (Ser473), total Akt, phosphorylated Erk1/2, total Erk1/2 (Cell Signaling Technologies, Danvers, MA, USA; all at 1:1000) and Hsc70 as a loading control (Enzo, Farmingdale, NY, USA, 1:1000). Membranes were developed using DylightTM-680 or DylightTM-800 conjugated secondary antibodies (1:20,000; Invitrogen, Carlsbad, CA) and visualised using the Odyssey Infrared Imaging system (LI-COR Bioscience, Lincoln, NE, USA).

C57BL/KaLwRij murine model of MM:

C57BL.KaLwRijHsd (KaLwRij) mice were bred and housed at the South Australian Health and Medical Research Institute (SAHMRI) Bioresources facility. All animal studies were approved by and performed in accordance with the SAHMRI Animal Ethics Committee (Ethics approval number SAM356). Five- to six-week-old female KaLwRij mice were inoculated into the left tibia with 1x10⁵ 5TGM1-CCR1 or control 5TGM1-EV cells in 10 μ L phosphate-buffered saline (PBS). After 25 days, mice were injected with firefly D-luciferin (150mg/kg, diluted in PBS, 100 μ L i.p.), anaesthetized and after 15 min PB was collected by cardiac puncture. Mice were then humanely killed, and spleens were dissected and immediately imaged using bioluminescent imaging (Xenogen IVIS 100; Perkin Elmer). Bioluminescence signal below background (2000 p/sec/cm²/sr) was classified as not detectable. PB was subjected to red cell lysis as described previously¹³ and resuspended in PBS with 2% FCS and 2mM EDTA (PFE) prior to analysis of GFP⁺ cells on a FACSCanto II flow cytometer (BD Biosciences). Injected tibiae, and tibiae and femora from the contralateral leg, were excised and BM was flushed with 10mL PFE and resuspended in 1mL PFE for analysis of GFP⁺ cells on a LSRFortessa flow cytometer. GFP⁺ tumour cells of total viable mononuclear (parent) cells below 0.01% was defined as not detectable.

NSG murine model of MM:

NOD.Cg-Prkdc^{scid} Il2rg^{tm1Wjl}/SzJ (NSG) mice were bred and housed at the SAHMRI Bioresources facility. All animal studies were approved by and performed in accordance with the SAHMRI Animal Ethics Committee (Ethics Approval Number SAM286). Female NSG mice (5-6 weeks old) were inoculated into the left tibia with 5×10^5 OPM2-EV-1 or OPM2-CCR1-KO-1 cells in 10 μ l PBS. After 28 days, long bones and PB were isolated and tumour burden, circulating tumour cells and soft tissue and bone dissemination was assessed as described for the C57BL/KaLwRij murine model of MM above. Spleens were excised, photographed and measured and were fixed in 10% neutral buffered formalin and paraffin embedded prior to immunohistochemistry analysis as described below.

For CCR1 inhibition studies with the CCR1 small-molecule inhibitor CCX9588, 5-6-week-old female mice were injected intra-tibially with 5×10^5 OPM2-EV-1 or RPMI-8226-luc cells. Mice were treated twice daily (12h intervals) via oral gavage with either CCR1 antagonist CCX9588 (15mg/kg) or PEG vehicle alone commencing either at 3 or 14 days after tumour-cell injection until day 28 at experimental endpoint. After 28 days, long bones and PB were isolated and tumour burden, circulating tumour cells and soft tissue and bone dissemination was assessed as described for the C57BL/KaLwRij murine model of MM above. For mice treated from day 3 post-tumour cell injection, blood from terminal cardiac bleeds was also used for performing total blood counts using a HEMAVET 950 automated blood analyser (Drew Scientific, Miami Lakes, FL, USA), and serum analysis of trough (12 hours after final dose) CCX9588 levels by liquid chromatography/mass spectrometry at ChemoCentryx (Mountain View, CA).

Immunohistochemistry:

Tumour cells in paraffin-embedded sections (5 μ m) were immunostained using a goat polyclonal anti-GFP antibody (Rockland, Pottstown, PA), biotinylated anti-goat secondary antibody (Vector Laboratories, CA, USA) followed by incubation with streptavidin-HRP (Vector Laboratories) and DAB (Vector Laboratories) as previously described.¹⁴

Statistical Analyses:

Univariate and multivariable analyses of factors associated with overall survival in microarray dataset E-TABM-1138 were conducted using IBM SPSS version 26. Initially, the proportional hazards assumption was tested and univariate Cox regressions were conducted to identify

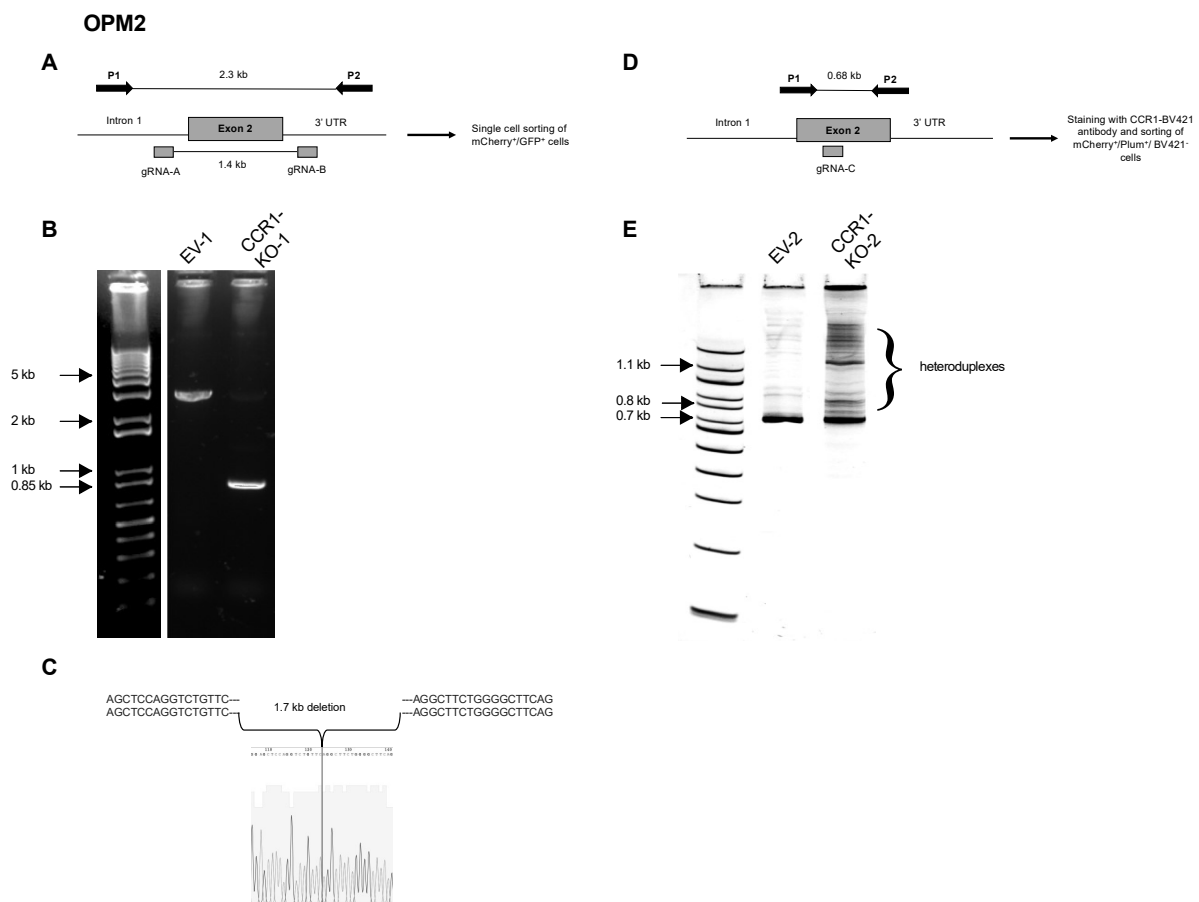
factors that were significantly associated with overall survival ($p < 0.1$). These factors were then included in a multivariable Cox proportional hazards model. All other statistical analyses were performed using GraphPad Prism 7 (GraphPad Software Inc., San Diego, CA, USA). Overall survival was analyzed using Kaplan-Meier curves and the log-rank test. *In vitro* assays were analyzed using unpaired t-test for comparisons between cell lines, two-way ANOVA with Sidak's multiple comparisons test for migration assays, or one-way ANOVA with Tukey's multiple comparisons test for WST-1 and viability assays. *In vivo* experiments were analyzed using a Mann-Whitney U test for tumour burden, one-way ANOVA with Tukey's multiple comparisons test for splenic size analysis, or a Fisher's exact test for incidence of dissemination.

References:

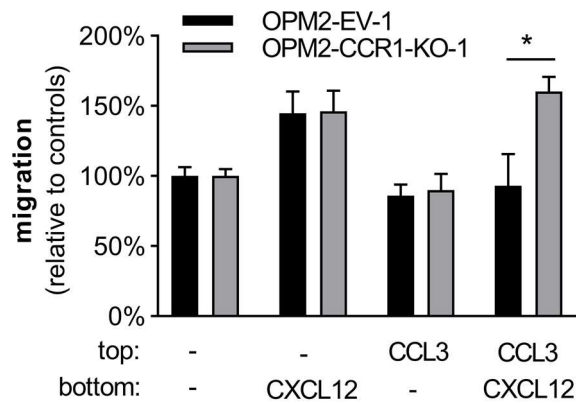
1. Zannettino ACW, Farrugia AN, Kortessidis A, et al. Elevated serum levels of stromal-derived factor-1 α are associated with increased osteoclast activity and osteolytic bone disease in multiple myeloma patients. *Cancer Res.* 2005;65(5):1700-1709.
2. Rajkumar SV, Dimopoulos MA, Palumbo A, et al. International Myeloma Working Group updated criteria for the diagnosis of multiple myeloma. *Lancet Oncol.* 2014;15(12):e538-548.
3. Vandyke K, Zeissig MN, Hewett DR, et al. HIF-2 α promotes dissemination of plasma cells in multiple myeloma by regulating CXCL12/CXCR4 and CCR1. *Cancer Res.* 2017;77(20):5452-5463.
4. Cheong CM, Chow AW, Fitter S, et al. Tetraspanin 7 (TSPAN7) expression is upregulated in multiple myeloma patients and inhibits myeloma tumour development in vivo. *Exp Cell Res.* 2015;332(1):24-38.
5. Diamond P, Labrinidis A, Martin SK, et al. Targeted disruption of the CXCL12/CXCR4 axis inhibits osteolysis in a murine model of myeloma-associated bone loss. *J Bone Miner Res.* 2009;24(7):1150-1161.
6. Weber K, Bartsch U, Stocking C, Fehse B. A multicolor panel of novel lentiviral "gene ontology" (LeGO) vectors for functional gene analysis. *Mol Ther.* 2008;16(4):698-706.
7. Hewett DR, Vandyke K, Lawrence DM, et al. DNA barcoding reveals habitual clonal dominance of myeloma plasma cells in the bone marrow microenvironment. *Neoplasia.* 2017;19(12):972-981.
8. Sena-Esteves M, Tebbets JC, Steffens S, Crombleholme T, Flake AW. Optimized large-scale production of high titer lentivirus vector pseudotypes. *J Virol Methods.* 2004;122(2):131-139.
9. Aubrey BJ, Kelly GL, Kueh AJ, et al. An inducible lentiviral guide RNA platform enables the identification of tumor-essential genes and tumor-promoting mutations in vivo. *Cell Reports.* 2015;10(8):1422-1432.
10. Livak KJ, Schmittgen TD. Analysis of relative gene expression data using real-time quantitative PCR and the 2 $^{-\Delta\Delta CT}$ Method. *Methods.* 2001;25(4):402-408.
11. Mrozik KM, Cheong CM, Hewett D, et al. Therapeutic targeting of N-cadherin is an effective treatment for multiple myeloma. *Br J Haematol.* 2015;171(3):387-399.
12. Fitter S, Dewar AL, Kostakis P, et al. Long-term imatinib therapy promotes bone formation in CML patients. *Blood.* 2008;111(5):2538-2547.

13. Opperman KS, Vandyke K, Clark KC, et al. Clodronate-liposome mediated macrophage depletion abrogates multiple myeloma tumor establishment in vivo. *Neoplasia*. 2019;21(8):777-787.
14. Fitter S, Matthews MP, Martin SK, et al. mTORC1 plays an important role in skeletal development by controlling preosteoblast differentiation. *Mol Cell Biol*. 2017;37(7):e00668-00616.

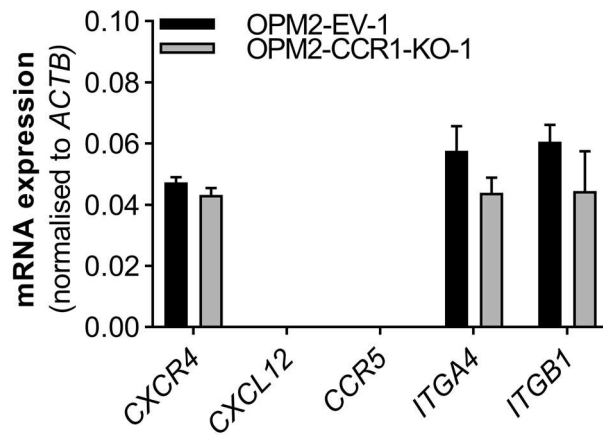
Supplementary Figures:



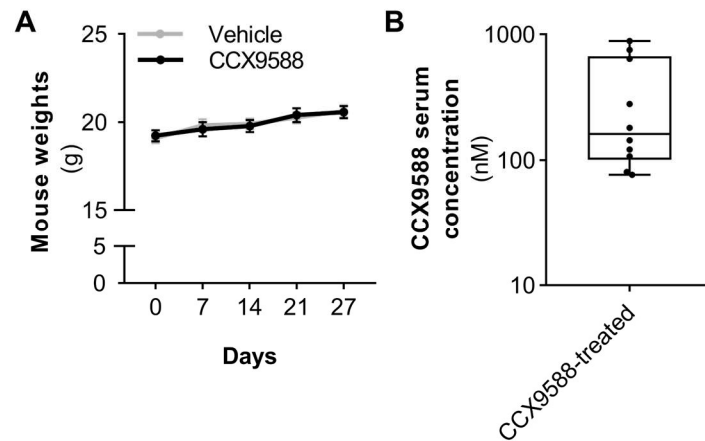
Supplementary Figure S1. Verification of OPM2 CCR1 knockout cell lines. **A.** Schematic diagram of CRISPR-Cas9 strategy OPM2 to generate CCR1-KO-1 cell line. P1 and P2 represent forward and reverse sequencing primers, respectively, and location of gRNA-A and -B binding sites are indicated. **B.** PCR to confirm CRISPR-Cas9 deletion of the CCR1 exon in OPM2-CCR1-KO-1 cells compared with non-deleted CCR1 sequence in OPM2-EV-1 cells. **C.** Sanger sequencing of OPM2-CCR1-KO-1 deletion band. **D.** Schematic diagram of CRISPR-Cas9 strategy OPM2 to generate CCR1-KO-2 cell line. P1 and P2 represent forward and reverse sequencing primers, respectively, and location of gRNA-C binding site is indicated. **E.** CRISPR-Cas9 mutagenesis of the CCR1 exon was confirmed in OPM2-CCR1-KO-2 cells compared with OPM2-EV-2 control cells.



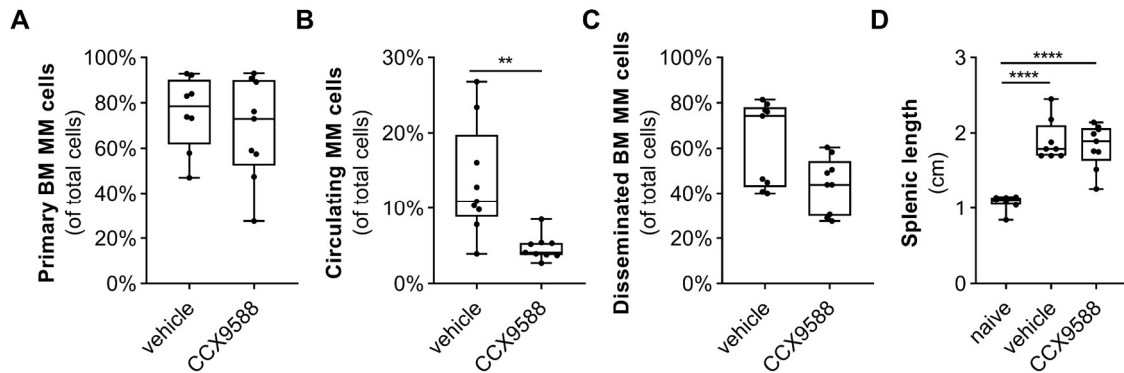
Supplementary Figure S2. CCL3 treatment does not affect migration of OPM2 CCR1 knockout cells towards CXCL12. OPM2-EV-1 or OPM2-CCR1-KO-1 cells were treated with 100 ng/mL rhCCL3 or media alone for 72 h, cells were washed, and migration towards 100 ng/mL rhCXCL12 was assessed. Migration towards rhCCL3 is expressed relative to the untreated control cells. Graph depicts mean \pm SEM of triplicates from a single experiment, * $p < 0.05$, two-way ANOVA with Sidak's post-test.



Supplementary Figure S3. Knockout of CCR1 in OPM2 cells does not result in a compensatory effect on chemokine receptor or adhesion molecule expression. mRNA expression of *CXCR4*, *CXCL12*, *CCR5*, *ITGA4* and *ITGB1* was assessed by real-time qPCR in OPM2-CCR1-KO-1 or control OPM2-EV-1 cells. Graph depicts mean \pm SEM of three independent experiments.



Supplementary Figure S4. Four-week treatment of NSG mice with twice daily treatment with the CCR1 inhibitor CCX9588 was well-tolerated *in vivo*. **A.** Weights of OPM2-tumor bearing NSG mice were treated with PEG vehicle or CCX9588 via twice daily oral gavage daily for 25 days. **B.** Trough serum concentrations of CCX9588 (C_{\min}) were measured 12 hours after the final dose in OPM2-tumor bearing CCX9588-treated NSG mice. Graph depicts mean \pm SEM, n=10-12 mice/group (**A**), median and interquartile range, n=10 mice (**B**).



Supplementary Figure S5. Targeting of CCR1 reduces circulating tumour cell numbers in NSG mice with established OPM2 tumour. **A.** Primary tumour burden is shown 4 weeks following intratibial injection of NSG mice with OPM2-EV-1 cells with treatment on days 14-28 with CCX9588 (15mg/kg) or vehicle control at 12-hour intervals. **B.** Number of circulating OPM2-EV-1 cells in peripheral blood of mice treated on days 14-28 with CCX9588 (15mg/kg) or vehicle control at 12-hour intervals. **C.** Disseminated tumour burden in the contralateral leg after 4 weeks in NSG mice injected with OPM2-EV-1 cells and treated on days 14-28 with CCX9588 (15mg/kg) or vehicle control at 12-hour intervals. **D.** Spleens collected from naïve NSG mice or vehicle- or CCX9558-treated mice bearing OPM2-EV-1 cells were measured to assess the degree of splenomegaly after 4 weeks. Naïve mice splenic sizes are duplicated from Figure 5D for ease of comparison. Box and whisker plots depict median and interquartile ranges, n=9 mice/group (**A-C**), n=7-9 mice per group (**D**). **p<0.01, Mann-Whitney test (**B**), ****p<0.0001, one-way ANOVA with Tukey's multiple comparison test (**D**).

Supplementary Table 1. Complete blood counts of OPM2-tumour bearing or naïve NSG¹ mice following 25-day CCX9588 treatment

Parameter	Naïve ² n=3	Vehicle ² n=10	CCX9588 ² n=9	<i>P</i> -value ³	<i>P</i> -value ⁴
White blood cells (K/ μ L)	1.66 \pm 0.39	1.94 \pm 0.15	2.06 \pm 0.23	>0.99	>0.99
Red blood cells (K/ μ L)	6.30 \pm 0.87	6.76 \pm 0.21	6.52 \pm 0.25	>0.99	>0.99
Haemoglobin (g/dL)	9.48 \pm 1.34	8.41 \pm 0.28	8.13 \pm 0.34	0.93	>0.99
Haematocrit (%)	33.18 \pm 4.78	34.37 \pm 1.15	32.89 \pm 1.27	>0.99	>0.99
Mean corpuscular haemoglobin (pg)	15.00 \pm 0.25	12.48 \pm 0.12	12.47 \pm 0.12	0.025	>0.99
Mean corpuscular haemoglobin concentration (g/dL)	28.62 \pm 0.49	24.49 \pm 0.27	24.71 \pm 0.14	0.035	>0.99
Platelets (M/ μ L)	863.0 \pm 242.3	524.3 \pm 34.67	492.6 \pm 64.34	0.68	>0.99

¹9-10 weeks of age at the time of cardiac bleed

²Mean \pm SEM

³Naïve versus vehicle; Kruskal-Wallis test with Dunn's post-test

⁴Vehicle versus CCX9588; Kruskal-Wallis test with Dunn's post-test